Mon. Not. R. Astron. Soc. **000**, 1–4 (0000) Printed 16 January 2016 (MN LATEX style file v2.2)

QSO selection

Martin White

16 January 2016

ABSTRACT

Details on how to convert from "intrinsic" properties of the mock QSO sample to observed properties, and then apply a model of the DESI selection function.

1 MOCK CATALOGS

This document describes some mock catalogs which can be used to develop the analysis pipeline and perform mission optimization for `DESI`. Here the focus is on converting from "intrinsic" to "observed" properties for a mock quasar catalog. We shall use as an example the `v1.0` catalogs described elsewhere.

The magnitudes in the mock catalog are stored as $M_i(z = 2)$, to conform to the convention most often used in SDSS and BOSS publications (though there are good reasons to modify this convention in the future: see Ross et al. (2013) for further discussion). To convert to M_{1450} one can use $M_{1450} \simeq M_i(z = 2) + 1.486$ and to convert to bolometric luminosity one can use $M_i(z = 2) = 72.5 - 2.5\lg L_{\rm bol}$ with the luminosity in Watts or $M_i(z = 2) = 90 - 2.5\lg L_{\rm bol}$ with the luminosity in erg s^{-1} (Shen et al. 2009). The catalog contains only QSOs above $M_i(z = 2) = -22$.

Figure 1 shows the simulated QLF compared to observations. The simulated QLF was computed by simply binning the mock QSOs in bins of absolute luminosity and dividing by the volume of the box. The observations have all been converted to $M_i(z = 2)$ and references are given in the figure caption.

The QSO boxes need to be projected into the survey geometry and passed through the appropriate masks etc. The projection and masking follows the same flow as any other target class, and can be accomplished using the `Box2Sky` code in `MockingDESI`. In order to be 'observed' the QSOs need to be selected as targets and then have an efficiency of getting a good spectrum. We shall consider this problem below.

2 QUASAR COLORS AND SELECTION

2.1 Methodology

The simplest way to 'select' the targets is to have a table of selection efficiency vs. luminosity and redshift and draw random numbers. A more sophisticated approach would generate mock colors for the QSOs and apply some color cuts. To generate mock colors for the QSOs we need several inputs: the power-law continuum (with variable slopes?) and IR emission, possible contribution from the host galaxy at low z and L, Lyα and Lyman-limit system absorption and emission lines. Several partial or more complete models exist for each of these components (see for example the discussion in Ross et al. 2013 among many possibilities). We could also use composite spectra (e.g. from SDSS or BOSS) or synthetic spectra or objects from existing template libraries (e.g. Budavari et al. 2001). In what follows we shall follow the simplest approach.

Redshift	χ	DM	K	$g-i$
0.50	1944.1	42.32	0.23	0.18
0.75	2726.6	43.39	0.24	0.16
1.00	3400.8	44.16	0.06	0.19
1.25	3983.9	44.76	-0.12	0.23
1.50	4491.7	45.25	-0.25	0.26
1.75	4937.3	45.66	-0.28	0.25
2.00	5331.5	46.02	-0.24	0.21
2.25	5682.7	46.33	-0.21	0.14
2.50	5997.9	46.61	-0.20	0.08
2.75	6282.6	46.86	-0.30	0.07
3.00	6541.3	47.09	-0.31	0.16
3.25	6777.6	47.30	-0.34	0.42
3.50	6994.5	47.49	-0.39	0.94

Table 1. Distance measures in our fiducial cosmology, a ΛCDM model with $\Omega_m = 0.3 = 1 - \Omega_\Lambda$, $h = 0.68$. The comoving radial distance, χ, is in Mpc. The $g - i$ color is determined by the polynomial fit given in the text.

2.2 g-band selection function

The probability that a QSO will receive a fiber (hereafter the selection function) for DESI can be well approximated as a function of g-band magnitude (N. Palanque-Delabrouille, private communication) with probability

$$P = (83 \pm 10)\% \qquad 00.0 < g < 22.0 \tag{1}$$

$$P = (72 \pm 15)\% \qquad 22.0 < g < 22.5 \tag{2}$$

$$P = (37 \pm 15)\% \qquad 22.5 < g < 23.0 \tag{3}$$

We use a simple linear fit to this function, setting $P = 0$ for $g > 23$. This requires us to convert from the absolute magnitude supplied by the mock catalog, $M_i(z = 2)$, to observed g-band magnitude.

2.3 K-correction

The relation between i-band apparent and absolute magnitude is (see e.g. Ross et al. 2013, for further discussion)

$$m = M_i(z = 2) + {\rm DM} + K \tag{4}$$

The distance modulus, DM, is defined as

$${\rm DM} = 25 + 5\log_{10}\left[\frac{(1+z)\chi}{\rm Mpc}\right] \tag{5}$$

with χ the comoving radial distance. We use the K-correction sign convention above, in agreement with most of the SDSS papers.

For a power-law continuum with slope α, the K-correction

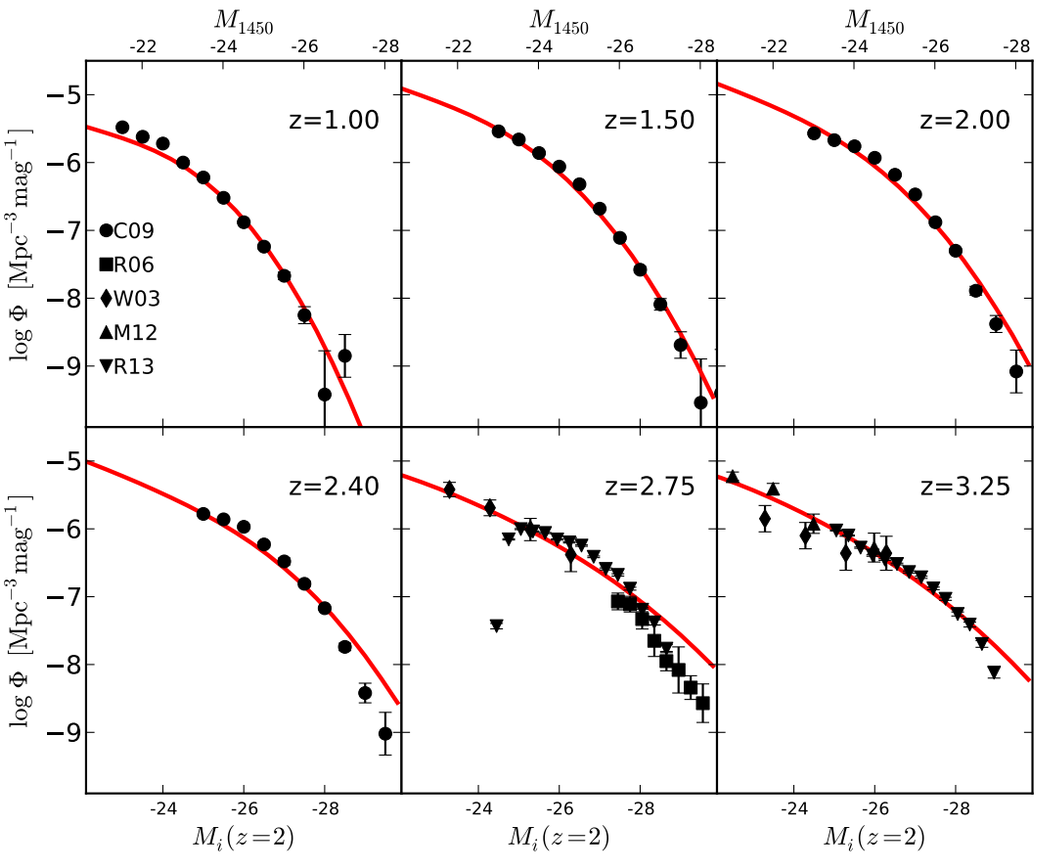

Figure 1. Comparison of the mock QLFs to observations at selected redshifts. In each panel the red line shows the histogram of the mock quasars in the simulation box, while the points with error bars show the data from Croom et al. (2009); Richards et al. (2006); Wolf et al. (2003); Masters et al. (2012); Ross et al. (2013), with all magnitudes converted to $M_i(z = 2)$ and M_{1450} as needed. For most data sets, the errors bars indicate only the statistical error. The simulations generally do a very good job of fitting the interpolated QLF, but for some redshifts (e.g. $z = 2.75$) the interpolated QLF has a hard time passing through all of the different data sets and picks a compromise solution. This figure is taken from `qso_mock.pdf` for the `v1.0` mocks.

Redshift	$c\chi^2/H$	Const
0.50	8.7	42.74
0.75	14.7	43.79
1.00	19.7	44.41
1.25	23.5	44.87
1.50	26.1	45.26
1.75	27.7	45.63
2.00	28.7	45.98
2.25	29.2	46.26
2.50	29.3	46.49
2.75	29.1	46.63
3.00	28.8	46.94
3.25	28.3	47.39
3.50	27.7	48.04

Table 2. The volume factor, $c\chi^2/H$, in 10^9 Mpc^3, and offset between apparent g-band magnitude and $M_i(z = 2)$ as a function of redshift.

would be $-2.5(1 + \alpha)\log_{10}[(1 + z)/(1 + 2)]$, where we have followed the SDSS QSO convention and corrected to $z = 2$ rather than $z = 0$. However the power-law approximation is not particularly good. Instead we use the tabulated K-correction of Richards et al. (2006). There is a newer K-correction in Ross et al. (2013), which is compared to the older, Richards et al. (2006), table in Ross et al. (2013, Fig. 9). However, the Ross et al. (2013) table does not extend below $z = 2$.

Assuming a power-law continuum and using the effective wavelengths of the filters, the transformation from i to g would be

$$M_g = M_i + 2.5\alpha \log_{10}\left(\frac{4670\,\text{Å}}{7470\,\text{Å}}\right) = M_i + 0.255 \qquad (6)$$

if we assume $\alpha = -0.5$. However, as for the K-correction, the power-law approximation is not particularly good. Fig. 2 shows the extinction corrected $g - i$ colors of spectroscopically confirmed QSOs from SDSS and BOSS in narrow bins of redshift. The horizontal, dotted black line shows $g - i = 0.255$ as above. The rise in $g - i$ color at high redshift is due to intergalactic absorption of shorter wavelength radiation leading to a 'break' in the spectrum which impacts the g-band flux. The solid black line shows a 4$^{\text{th}}$ order polynomial fit to the medians of the distribution

$$g - i = 0.1502\,z^4 - 0.9886\,z^3 + 2.147\,z^2 - 1.758\,z + 0.6397 \qquad (7)$$

As with all polynomial fits, it should not be extrapolated outside of the range of the fit ($0.5 < z < 3.5$). Table 1 gives the radial

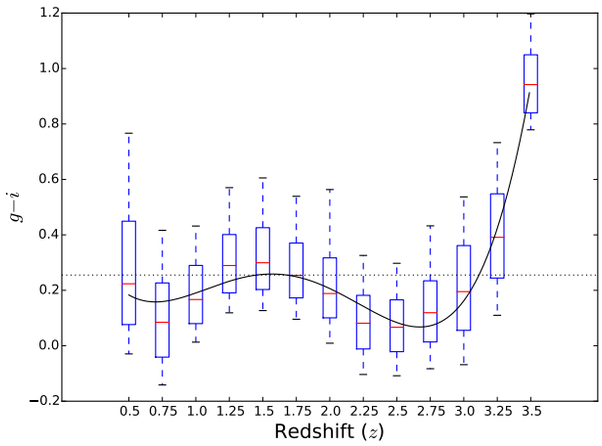

Figure 2. A box-and-whisker plot showing the $g-i$ color of SDSS (DR7) and BOSS (DR12) quasars in bins of redshift (of width ±0.01). The central, horizontal line, in each box shows the median color with the box spanning the quartiles and the end caps showing the 10$^{\rm th}$ to 90$^{\rm th}$ percentiles. The dotted line shows $g-i=0.255$ as in Ross et al. (2013) while the solid line shows the 4$^{\rm th}$ order polynomial fit to the medians given in the text.

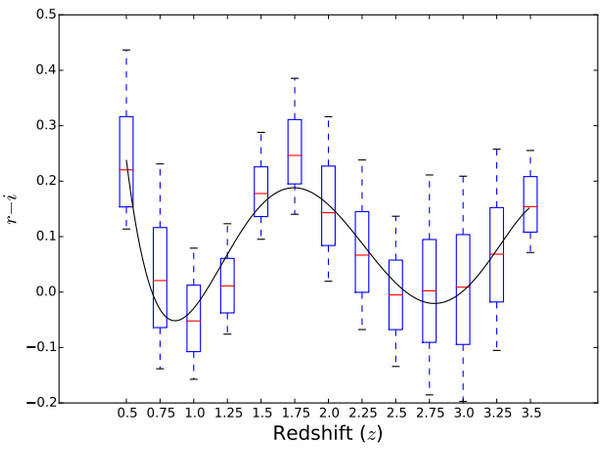

Figure 3. A box-and-whisker plot showing the $r-i$ color of SDSS (DR7) and BOSS (DR12) quasars in bins of redshift (of width ±0.01). The central, horizontal line, in each box shows the median color with the box spanning the quartiles and the end caps showing the 10$^{\rm th}$ to 90$^{\rm th}$ percentiles. The solid line shows the 4$^{\rm th}$ order polynomial fit to the medians given in the text.

distance (χ) distance modulus (DM) K-correction (K) and median color ($g-i$) as a function of redshift for a 'fiducial' ΛCDM model with $\Omega_m=0.3$ and $h=0.68$.

2.4 Counts

To convert from the intrinsic properties and luminosity function to counts per square degree we make use of the fact that for a flat, Friedmann model

$$\frac{dV}{dz\,d\Omega}=\frac{c\chi^2}{H} \tag{8}$$

with H the Hubble parameter at the observed redshift. Since at fixed z the apparent magnitude is simply shifted from the absolute magnitude by a constant, the counts per unit redshift, per unit magnitude, per solid angle are

$$\frac{dN}{dm\,dz\,d\Omega}=\frac{c\chi^2}{H}\,\Phi(M=m-\text{const}) \tag{9}$$

We list the volume prefactor, $c\chi^2/H$, and the constant offset [DM + K + $(g-i)$] between apparent g-band magnitude and absolute i-band magnitude [i.e. $M_i(z=2)$] in Table 2 for our fiducial cosmology and using the 4$^{\rm th}$ order polynomial fit to $g-i$.

Fig. 4 compares the counts predicted by the mock catalog to those in `desimodel/trunk/data/targets/dNdzdg_QSO.dat`. Counts are given per redshift interval, per g-band magnitude and per square degree as a function of g-band magnitude in several redshift bins.

3 HIGH-Z COUNTS

Overall the agreement between the mock-predicted counts and `dNdzdg_QSO.dat` is quite good. However there are discrepancies at the highest redshift. To cross-check these points we compare the high z QLF from the constant-time mock box to a compilation of data (as in Fig. 1) at $z=3.75$. Overall the agreement is very good. This suggests that one of our interpolations or the conversion from $M_i(z=2)$ to apparent g-band magnitude is in error. We have not been able to identify the approximation which is causing the shortfall. To get a feel for the size of the correction we would need to bring the counts into agreement, we show in the last panel of Fig. 4 the mock counts shifted 'left' by 1.25 magnitudes.

4 RED SELECTION

The 'default' selection band for QSOs in DESI is r-band, rather than g-band, because the g-band is so affected by absorption for high z QSOs. Fig. 3 shows the distribution of $r-i$ colors as a function of z, estimated in the same way as for Fig. 2. The solid line is the 5$^{\rm th}$ order polynomial

$$r-i=-0.1482\,z^5+1.636\,z^4-6.716\,z^3+12.55\,z^2-10.39\,z+3.017 \tag{10}$$

Note that over most of the range plotted this polynomial gives numbers $O(0.1)$ even though the coefficients are $O(1)$ so significant cancellation is going on and extrapolation is even more disfavored than usual.

Note: Both the g- and r-band apparent magnitude are provided in the catalogs, to aid in determining which objects would be selected or what the S/N of the spectrum might be, but these relations are purely deterministic from $M_i(z=2)$. Thus there is no information on per-QSO color that can be obtained from these fields.

5 LIGHTCONES

The constant-time boxes, spaced every $\Delta z=0.25$, are then combined into light-cone outputs using the `MockingDESI` software. Since the QLF evolves strongly across the redshift range of interest we linearly interpolate the data in each box. Specifically an object in a specific output is selected with probability $1-(z-z_{\rm out})/\Delta z$, where $z_{\rm out}$ is the redshift of the output. The light-cone catalog is simply the catenation of the selected objects for every box.

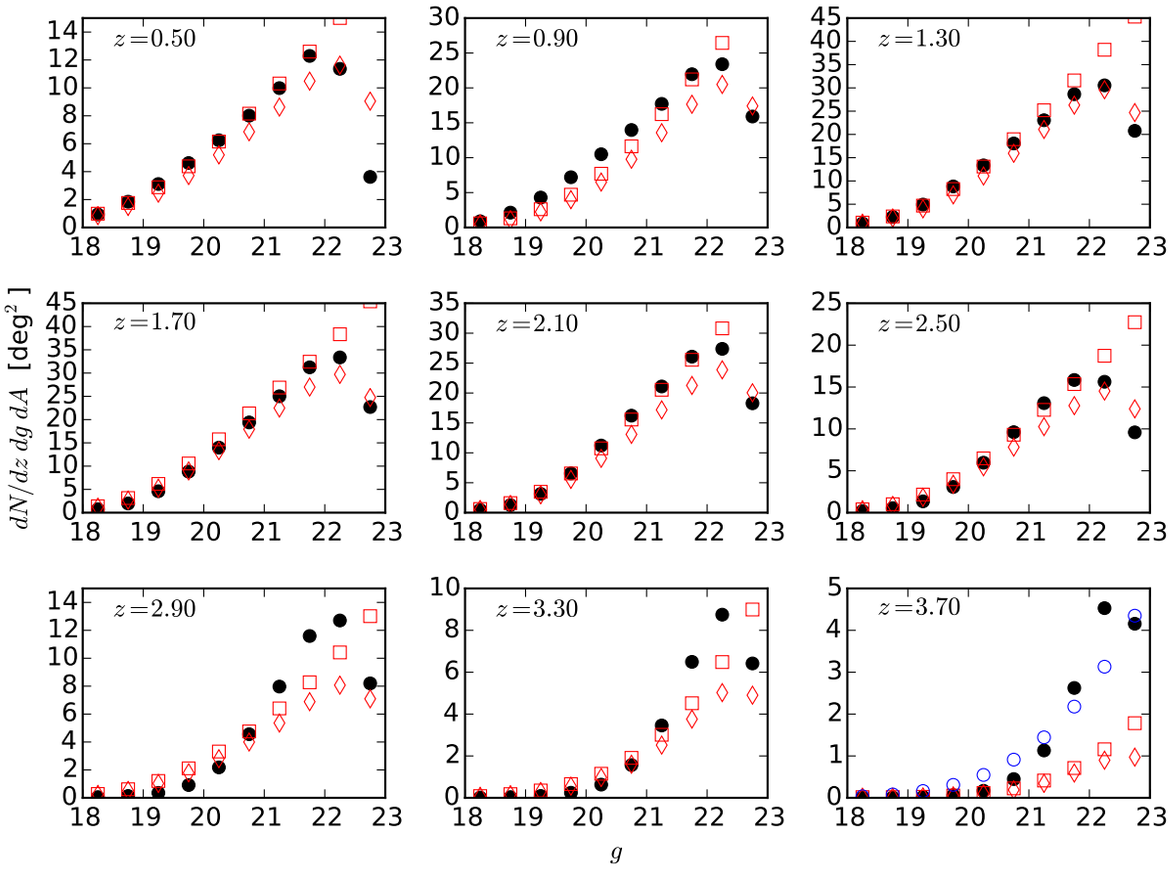

Figure 4. Comparison of the counts predicted by the mock catalogs to those in `desimodel/trunk/data/targets/dNdzdg_QSO.dat` at selected redshifts. In each panel the solid black circles show the values from `dNdzdg_QSO.dat`, multiplied by 10 to get QSOs per unit redshift, per unit magnitude, per square degree. The open (red) squares show the counts predicted from the mock QLF assuming the volume factors and magnitude offsets of Table 2. The open (red) diamonds show those results multiplied by a linear interpolation of the selection function given in §2.2. The blue points in the last panel show the counts if the magnitudes are shifted by 1.25, as discussed in the text.

REFERENCES

Behroozi, P., Conroy, C., Wechsler, R.H., 2010, ApJ, 717, 379
Budavari, T., Csabai, I., Szalay, A., et al., 2001, AJ, 122, 1163
Conroy, C., & White, M. 2013, ApJ, 762, 70
Croom, S. M., Richards, G. T., Shanks, T., et al. 2009, MNRAS, 399, 1755
Masters, D., Capak, P., Salvato, M., et al. 2012, ApJ, 755, 169
Moster, B., Naab, T., White S.D.M., 2013, MNRAS, 428, 3121
Palanque-Delabrouille N., et al., 2015, preprint [arxiv:1509.05607]
Richards, G. T., Strauss, M. A., Fan, X., et al. 2006, AJ, 131, 2766
Ross N. P., Shen Y., Strauss, M. A., et al. 2009, ApJ, 697, 1634
Ross, N. P., McGreer, I. D., White, M., et al. 2013, ApJ, 773, 14
Shen, Y., Strauss, M. A., Ross, N. P., et al. 2009, ApJ, 697, 1656
White, M., Myers, A. D., Ross, N. P., et al. 2012, MNRAS, 424, 933
Willott, C. J., Delorme, P., Reylé, C., et al. 2010, AJ, 139, 906
Wolf, C., Wisotzki, L., Borch, A., et al. 2003, AAP, 408, 499

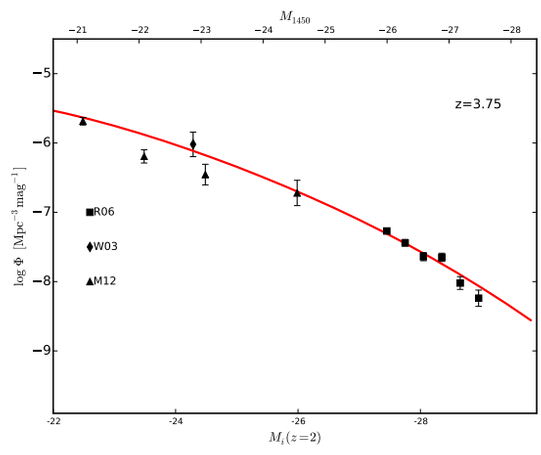

Figure 5. A comparison of the constant-time mock and a compilation of QLF measurements at z = 3.75.